MODESTUM
OPEN ACCESS
Eurasian Journal of Analytical Chemistry
ISSN: 1306-3057
2018 13(3):em23
DOI: 10.20933/ejac/81809

Novel Au–Fe_3O_4 NPs Loaded on Activated Carbon as a Green and High Efficient Adsorbent for Removal of Dyes from Aqueous Solutions: Application of Ultrasound Wave and Optimization

Saideh Bagheri [1], Hossein Aghaei [1*], Majid Monajjemi [1], Mehrorang Ghaedi [2], Karim Zare [1]

[1] Department of Chemistry, Science and Research Branch, Islamic Azad University, Tehran, P.O. Box 14515-755, Tehran, IRAN
[2] Chemistry Department, Yasouj University, Yasouj 75918-74831, IRAN

Received 01 October 2017 ▪ Revised 04 January 2018 ▪ Accepted 05 January 2018

ABSTRACT

Present study is devoted on the development of the effective methodology for removal ultrasonic to simultaneous removal of Bismarck Brown (BB) and Thymol Blue (TB) onto Au–Fe_3O_4 nanoparticles loaded on activated carbon (Au–Fe_3O_4-NPs-AC) in aqueous solution. The Au–Fe_3O_4-NPs-AC were synthesized and characterization by different techniques such as XRD, FE-SEM and FT-IR. The process efficiency was confirmed through examination of variables like initial BB and TB concentration (X1, X2, respectively), pH (X3), adsorbent mass (X4) and sonication time (X5). The optimum operating parameters (OOP) were evaluated by Response Surface Methodology (RSM) based on central composite design (CCD) for prediction and simulation of removal of BB and TB dye, while analysis of variances (ANOVA) give the estimate of significance of experimental variables. The experimental equilibrium data were fitted to the conventional isotherm models and accordingly Langmuir isotherm has good applicability for the explanation of experimental data with maximum monolayer capacity (Qmax) of 80 and 76.38 mg g-1 in binary system for BB and TB, respectively. Kinetic evaluation of experimental data showed that the BB and TB adsorption processes followed well pseudo-second-order and intraparticle diffusion models. The results of this study will be useful for further development of magnetic nanostructures for environmental applications.

Keywords: Au–Fe3O4-NPs-AC, dye, central composite design, response surface methodology, ultrasonicated adsorption

INTRODUCTION

Industries, such as leather, textile, dye stuffs, tanning, plastics, rubber and cosmetics generate huge amounts of synthetic dyes and pigments [1] and accordingly approximately 15% of total dyes release in to the wastewater. Disposal of colored textile wastewater in to the environment, without efficient treatment, imposes serious damages to aquatic life. Furthermore, some dyes (especially reactive dyes) are recalcitrant, non-biodegradable [2], stable to oxidizing agents [3], and toxic and mutagenic [4, 5]. AC despite of its porous structure and reasonable surface area supply low adsorption capacity and high cost which simply overcome these and process were accelerated loading, nanostructure material simply simply on its surface [6–9]. This modification can significantly increase the removal percentage and its adsorption capacity due to the increase in surface area and number of reactive sites. Ultrasound irradiation is unique accelerator of chemical process due to the phenomenon of acoustic cavitation, formation, growth and collapse of micrometrical bubbles as consequence of propagation of a pressure wave through liquid [10, 11]. Secondary effect of ultrasound namely cavitation (nucleation, growth and transient collapse of tiny gas bubbles) improve the mass transfer through convection pathway that is emerged from physical phenomena is consequence of micro-streaming, micro-turbulence, acoustic (or shock) waves and micro jets without significant

✉ s_bagheri2010@yahoo.com ✉ hn_aghaei@yahoo.com **(*Correspondence)**
✉ m_monajjemi@yahoo.com ✉ m_ghaedi@mail.yu.ac.ir ✉ kmzare@gmail.com

Table 1. Experimental factors, levels and matrix of CCD

Factors	Levels			Star pointα = 2.0	
	Low (-1)	Central (0)	High(+1)	-α	+α
(X_1) TB Concentration (mg L^{-1})	6	10	14	2	18
(X_2) BB Concentration (mg L^{-1})	6	10	14	2	18
(X_3) pH	2.0	6.0	10.0	2.0	10.0
(X_4) Adsorbent mass (g)	0.020	0.025	0.030	0.015	0.0355
(X_5) Sonication timemin)	3.0	4.0	5.0	2.0	6.0

change in equilibrium characteristics of the adsorption/desorption system [12]. Shock waves have the potential of creating microscopic turbulence within interfacial films surrounding nearby solid particles [13]. Acoustic streaming induced by the sonication is the movement of the liquid is conversion of sound to the kinetic energy which is known as useful tool in intensifying the mass transfer process and breaking the affinity between adsorbate and adsorbent [14, 15]. Ghaedi et al. [16-19, 20, 21] studied dyes removal using nanomaterial-loaded activated carbon whith more efficiency than the AC due to improvement in the interface area and number of interface reactive atoms. Metallic nanostructures such as NiSe and ZnSe nanoparticles, [17] Pt nanoparticles, [18] ZnS:Cu nanoparticles [20] and Cd(OH)2 nanowires [21] easily loaded on AC via their binding to OH and COOH present at the interface of AC which causes high improvement in the interface area and adsorbate- adsorbent interaction. The main objectives of present work is development of novel approach based on simultaneous application of ultrasound and Au –Fe3O4-NPs-AC for safe and clean removal of dyes through optimization of various operating parameters using CCD. The adsorbent was characterized by field emission scanning electron microscopy (FESEM), Fourier transform infrared spectroscopy (FTIR) and X-ray diffraction (XRD) and finally experimental equilibrium and kinetic of adsorption process were studied.

EXPERIMENTAL

Materials and Methods

The chemicals including Bismarck Brown and Thymol Blue, activated carbon, $FeCl_3.6H_2O$, $FeCl_2.4H2O$, NH_3, sodium citrate, $HAuCl_4$, NaOH and HCl with the highest purity available were purchased from Merck Co. (Darmstadt, Germany). An accurately weighted amount of dyes (BB and TB) were dissolved in deionized water to prepare 100 mg L^{-1} as to stock solution, while the working solutions were prepared by diluting this solution. A pH meter (Metrohm model-728) was adjusted for the pH measurement. Ultrasonic Homogenizer (UHP-400) (made in Ultrasonic Technology Development company-Iran) was used for the ultrasound-assisted. Dye concentrations were analyzed by measuring the absorbance using a Jasco UV–Vis spectrophotometer. All the instruments used in this work for the characterization purpose were fully described in our previous publications [22].

Ultrasound Assisted Adsorption Method

A batch process was applied to evaluate the adsorption performance of dyes from aqueous solutions in the presence of ultrasound. Adsorption experiments were carry out in a cylindrical glass vessel by addition of adsorbent (25 mg) into 50 mL of dyes solution at known concentrations (12 mg L^{-1} for both dye) and pH 6 with a known amount of adsorbent (0.025 g) and sonication time (5 min) at the room temperature. At the end of the adsorption experiments, the sample was immediately centrifuged and analyzed. The efficiency of dyes removal was determined at different experimental condition according to CCD method. The BB and TB removal (R%) and adsorbed dye amount (qe (mg g^{-1})) in the aqueous solution by Au-Fe_3O_4 -NPs-AC were computed according to well-known [22].

Statistical Analysis

The experimental results of the central composite design (CCD) were analyzed using STATISTICA 10.0 software (State-Ease Inc., Minneapolis, USA) and the optimal while RSM was applied for modeling and the optimization of effects of concentration of initial BB and TB concentration (X1 , X2 respectively), PH (X3), amount of adsorbent (X4) and contact time (X5) on the ultrasonic-assisted adsorption of BB and TB by Au-Fe_3O_4NPs-AC. Five independent variables were set at five levels at which the R% of BB and TB the response was determined and shown in **Table 1**. Analysis of variance (ANOVA) was carried out to evaluate the important and effective terms for modeling the response based on F-test and p-values [23, 24].

Table 1 (cont). Experimental factors, levels and matrix of CCD

Experiment	X1	X2	X3	X4	X5	R %BB	R %TB
1	14	6	4	0.03	5	89.6	100
2	6	14	8	0.02	3	89.49	85
3	6	6	8	0.03	3	93.6	90
4	6	14	8	0.02	5	92.54	85.45
5	14	6	4	0.02	5	86.5	97
6	14	14	8	0.02	5	85.71	90.15
7	14	14	4	0.02	5	92.58	95.5
8	14	14	8	0.02	3	80	81.92
9	10	10	6	0.035	4	96.79	98.66
10	6	6	8	0.02	5	95.87	95
11	10	10	2	0.025	4	90	92
12	10	10	6	0.015	4	85	90
13	14	6	8	0.02	5	72.26	95.5
14	14	6	4	0.03	3	90	92
15	10	10	6	0.025	4	99.65	97
16	14	14	4	0.02	3	88.18	89.24
17	14	6	4	0.02	3	85	89
18	6	14	8	0.03	5	93.48	90
19	14	6	8	0.03	5	80	99.8
20	14	14	4	0.03	3	92	91.38
21	6	14	8	0.03	3	98.5	92.8
22	14	14	4	0.03	5	95.31	96
23	10	10	6	0.025	4	99.8	98.7
24	14	6	8	0.03	3	80.73	95.6
25	6	6	8	0.03	5	97.56	97
26	10	10	10	0.025	4	87	85.42
27	10	18	6	0.025	4	95	100
28	10	10	6	0.025	4	99.5	98.18
29	6	6	4	0.03	3	93.7	92.35
30	6	6	8	0.02	3	88.78	90
31	14	14	8	0.03	3	90.42	89.65
32	2	10	6	0.025	4	100	99.62
33	10	12	6	0.025	2	90	90.75
34	14	6	8	0.02	3	67.99	85
35	6	14	4	0.02	3	90.75	93.89
36	6	14	4	0.02	5	96.6	95.43
37	6	6	4	0.02	5	95.81	95.44
38	10	10	6	0.025	4	98	96.43
39	10	10	6	0.025	4	100	99.12
40	6	6	4	0.03	5	98.51	99.36
41	18	10	6	0.025	4	74.24	98.59
42	10	10	6	0.025	4	100	98.11
43	6	14	4	0.03	3	92.8	95.31
44	10	10	6	0.025	6	100	100
45	6	6	4	0.02	3	90.6	94.25
46	6	14	4	0.03	5	96.8	97.08
47	10	10	6	0.025	4	99.35	97.14
48	14	14	8	0.03	5	95.42	98.02
49	10	2	6	0.025	4	93	90
50	10	10	6	0.025	4	99.6	100

Preparation of Au-Fe_3O_4 -NPs-AC

At first step, The $FeCl_3.6H_2O$ and $FeCl_2.4H_2O$ salts (molar ratio of Fe^{3+}: Fe^{2+}= 2:1) were dissolved in 200 mL pure water. Temperature of solution adjusted to 80ºC. Then while stirring and under nitrogen gas atmosphere and NH_3 (aq) (25%) were drupelet added to the solution of metallic ions. the solution was stirred for 2 h at 80ºC under N_2. Following this, the color of the bulk solution changed from orange to black. The black Fe_3O_4 NPs were separated

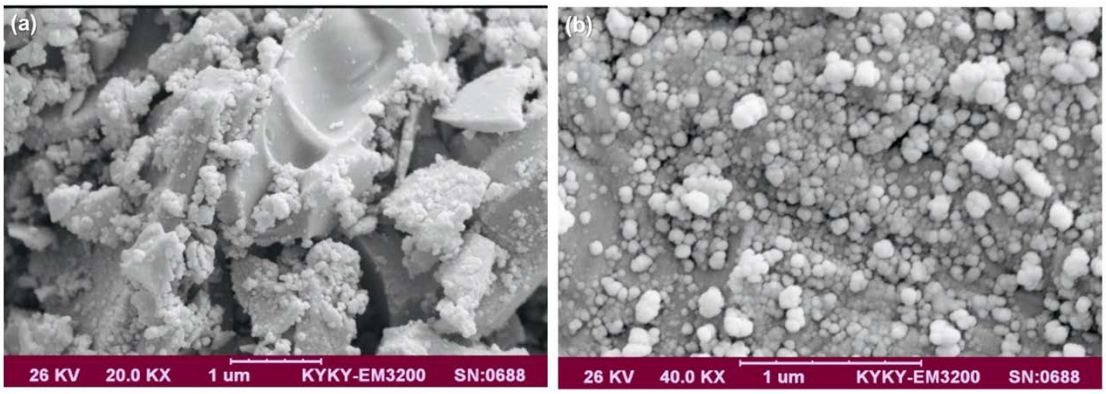

Figure 1. SEM image of (a) Fe3O4 -NPs-AC and (b) Au-Fe3O4 -NPs-AC

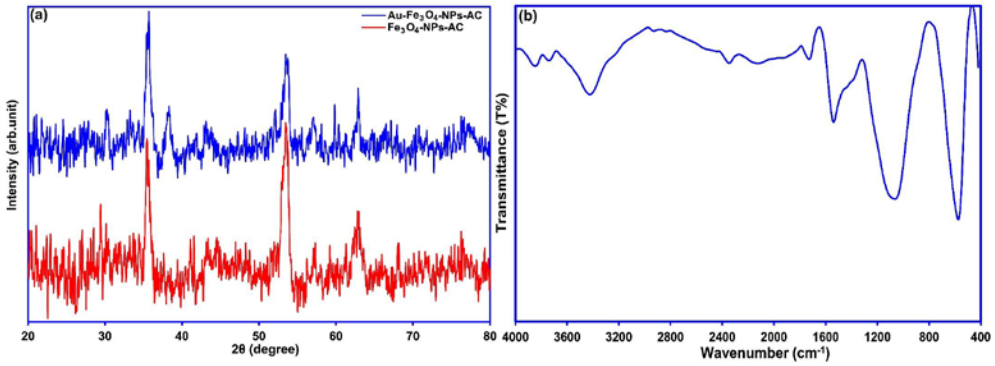

Figure 2. (a) XRD pattern and (b) FT-IR transmittance spectrum of the prepared Au-Fe3O4 -NPs-AC

by an external permanent magnet. The precipitates were washed several times with deionized water and ethanol. The synthesized Fe_3O_4 nanoparticles were dried in 70ºC. At two- step, in order to loaded Fe_3O_4 nanoparticles on carbon active, 2g carbon active was added 200 ml ethanol and sonicated for 1 h. then 0.4g Fe_3O_4 nanoparticles was add to mixture, while mixture was sonicated. Subsequence, prepared mixture was stirred for 20 h. The obtained products were filtrated, washed and collected, then dried in a hot air oven at in 70 ºC for 12 h. Finally the dried precipitate was grinded into powder form. Three- step, The Au NPs were synthesized by reducing $HAuCl_4$ with sodium citrate as reducing and stabilizer. Briefly, the 0.0625 mmol $HAuCl_4$ was heated with vigorous stirring until boiling. Addition 10 mL solution of 40 g/L sodium citrate resulted in a continuous color change from colorless to red and stirring continued for an additional 10 min after the color change ceased. The heating source was then removed and stirring continued for 10 min. After the solution cooled to room temperature. Then decorated carbon active with Fe_3O_4 nanoparticles was add to solution of Au nanoparticles and was sonicated for 30 min. Subsequence, prepared mixture was stirred for 20h. The obtained products were filtrated, washed and collected, then dried in 85 ºC for 16 h. and finally used as an absorbent for adsorption experiments.

RESULTS AND DISCUSSION

Characterization of Au-Fe_3O_4 -NPs-AC

The morphological studied by SEM are shown in (**Figure 1a** and **b**) denote uniform size, which in addition to its porous structure with high surface area making it suitable for the adsorption of target compounds. The structural analysis of the Au-Fe_3O_4NPs loaded on activated carbon by X-ray diffractometer (XRD) (**Figure 2a**). show peaks at 2θ = 35.2, 41.1, 52.8, 57, 62.4 ° and 67.1 belong to the lattice planes of (311), (400), (422), (511), (440), and (222) and confirm the cubic structure of Au-Fe_3O_4NPs loaded on activated carbon, respectively. The observed XRD peaks (**Figure 2a**), indicate well-crystalized structure of the Au-Fe_3O_4NPs -AC characteristic peaks correspond to impurities such as Fe, Au, $Fe(OH)_2$ and $Fe(OH)_3$ and/or other compounds. Fourier transform infrared spectroscopic analysis of Au-Fe3O4 –AC (**Figure 2b**), shows absorption peak at 1715 cm^{-1} assign to the stretching vibration of carbonyl groups. The broad peaks at 1180 cm^{-1} originated from C–O stretching and to C–C bonds. The broad absorption band at 3456 indicates the presence of surface hydroxyl groups (O–H stretching) and the bands at low wave numbers (≤700) are related to vibrations of the Fe–O and Au–O bonds in adsorbent. These functional groups may act as anchoring sites for dye molecules as reported in the literature [25].

Table 2. Analysis of variance (ANOVA) for R% of TB and BB

Source of variation	Df	TB				BB			
		Sum of square	Mean square	F-value	P-value	Sum of square	Mean square	F-value	P-value
Model	20	4813.0	240.65	18.880	< 0.0001	682.04	34.102	18.987	< 0.0001
X_1	1	820.36	820.36	64.360	< 0.0001	0.00090018	0.00090018	0.00050120	0.98229
X_2	1	257.99	257.99	20.241	0.00010182	125.20	125.20	69.710	< 0.0001
X_3	1	0.018714	0.018714	0.0014682	0.96970	10.984	10.984	6.1156	0.019503
X_4	1	973.51	973.51	76.376	< 0.0001	137.39	137.39	76.498	< 0.0001
X_5	1	88.569	88.569	6.9486	0.013332	64.521	64.521	35.924	< 0.0001
X_1X_2	1	137.37	137.37	10.777	0.0026832	25.152	25.152	14.004	0.00080179
X_1X_3	1	35.280	35.280	2.7679	0.10695	0.10928	0.10928	0.060844	0.80691
X_1X_4	1	306.90	306.90	24.078	< 0.0001	0.45840	0.45840	0.25523	0.61723
X_1X_5	1	0.026450	0.026450	0.0020751	0.96398	0.029403	0.029403	0.016371	0.89907
X_2X_3	1	13.261	13.261	1.0404	0.31616	5.4368	5.4368	3.0271	0.092490
X_2X_4	1	62.776	62.776	4.9250	0.034451	63.535	63.535	35.375	< 0.0001
X_2X_5	1	20.480	20.480	1.6067	0.21503	1.3001	1.3001	0.72386	0.40185
X_3X_4	1	10.306	10.306	0.80853	0.37596	8.0501	8.0501	4.4821	0.042950
X_3X_5	1	1.7205	1.7205	0.13498	0.71599	1.2129	1.2129	0.67532	0.41791
X_4X_5	1	12.350	12.350	0.96895	0.33309	8.0702	8.0702	4.4933	0.042709
X_1^2	1	9.3010	9.3010	0.72970	< 0.0001	2.6924	2.6924	1.4990	0.23067
X_2^2	1	46.397	46.397	3.6401	< 0.0001	0.15098	0.15098	0.084060	0.77393
X_3^2	1	42.532	42.532	3.3368	0.00010182	0.14607	0.14607	0.081329	0.77753
X_4^2	1	2.9113	2.9113	0.22840	0.96970	24.707	24.707	13.756	0.00087629
X_5^2	1	60.423	60.423	4.7404	< 0.0001	60.385	60.385	33.621	< 0.0001
Residual	10	369.64	240.65			52.085	1.7960		
Lack of Fit	1	301.45	12.746	1.4066	0.16246	46.688	2.1222	2.7525	0.086168
Pure Error	9	68.192	13.702			5.3970	0.77100		
Cor Total	30	5182.7				734.13			

Analysis of Central Composite Design

Central composite design (CCD) under RSM was applied to design a systematic series of experiments (50 runs) in five level. RSM makes it possible to nonlinearly model the experimental data [26-28]. The CCD avoids running unnecessary experiments while is useful for to understanding the synergies amongst the variables while supply value about interaction between the parameters. The analysis of variance (ANOVA) was performed to determine the level of significance of each term (**Table 2**).

$$R_{BB} = 99.018 - 6.7290X_1 + 3.2493X_2 - 4.2080X_3 + 5.3355X_4 + 3.8140X_5 + 4.5872X_1X_2 - 5.1675X_1X_3 + 2.5679X_1X_4 - 0.95248X_1X_5 + 3.6788X_2X_3 - 0.50336X_2X_4 + 1.5375X_2X_5 + 4.7161X_3X_4 - 0.13503X_3X_5 - 1.0939X_4X_5 - 6.7661X_1^2 - 1.0951X_2^2 - 10.649X_3^2 - 8.2536X_4^2 - 4.1486X_5^2 \quad (1)$$

$$R_{TB} = 98.176 + 0.019112X_1 - 1.5522X_2 - 3.5335X_3 + 3.9691X_4 + 4.9135X_5 - 0.61662X_1X_2 + 2.6765X_1X_3 + 1.5204X_1X_4 + 3.4303X_1X_5 - 2.2660X_2X_3 + 0.49292X_2X_4 - 1.0960X_2X_5 + 4.3253X_3X_4 + 0.37379X_3X_5 + 0.76027X_4X_5 + 0.83161X_1^2 - 5.1452X_2^2 - 8.9166X_3^2 - 3.2966X_4^2 - 2.2516X_5^2 \quad (2)$$

In this equation, the positive values correspond to each term indicate their positive effect on response and their negative values show a decrease in the response following raising their value. Analysis of variance (ANOVA) is a statistical method that partitions the total variation into its parts while each term has the different source of variation [29]. The interaction effects are easily estimated and by usual ANOVA, based on results presented in (**Table 2**), while the calculation is based on a sum of the squares which applied for estimation of factors effect and Fisher's F-ratios and P-values. The model F-value of 18.880 and 18.987 implied it's statistically significant and reveal that only 0.01% chance that ''model F-value" could happen due to noise. The non-significant value of lack of fit (more than 0.05) represents validity of the quadratic model for explanation of experimental data of present study [30].

Response Surface Plots (3D Surfaces)

RSM was then applied for improving the optimization and evaluation of the relative significance and interaction of variables on adsorption processes. The three- dimensional surface response plots of this interaction are shown in **Figure 3** and **4**, which demonstrate the interaction of TB concentration and pH with sonication time. Maximum

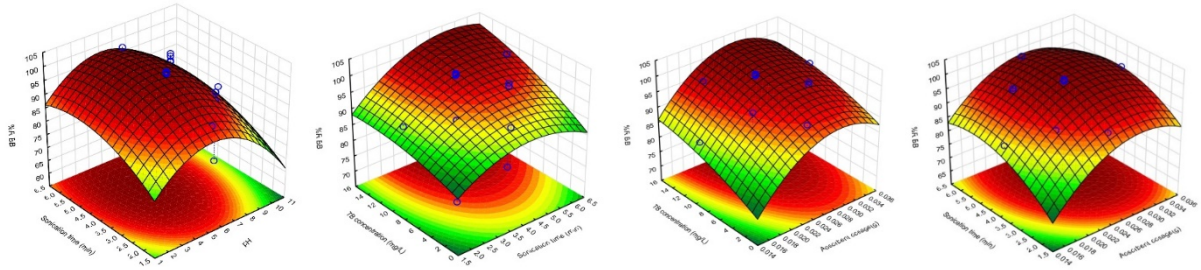

Figure 3. Response surfaces for the dyes removal: (a) pH -Sonication time, (b) initial TB concentration– Sonication time, (c) initial TB concentration– adsorbent dosage, (d) Sonication time – adsorbent dosage

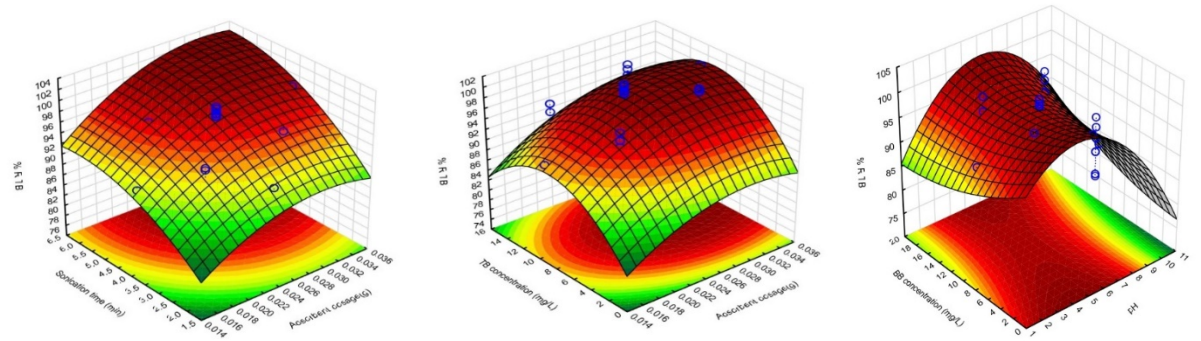

Figure 4. Response surfaces for the dyes removal: (a) Sonication time – adsorbent dosage; (b) initial TB concentration – adsorbent dosage, (c) BB concentration - pH

of dyes adsorption is achieved at high sonication times, which confirms the strong association between ultrasound and mass transfer. The results show that the initial adsorption rate is very rapid which emerged from the high available surface area and vacant sites s, while (**Figure 3c-d**) and (**Figure 4a**) increase in the adsorbent dose leads to a significant decrease in sonication time. On the other hand, the under study percentage dyes removal increases at higher adsorbent mass for particular sonication time. **Figure 4a-b** indicate the effect of pH with initial BB concentration, which show that pH has the negative correlation with removal percentage and higher pH led to the achievement of lower removal percentage. At low initial pH, protonation of the adsorbent functional groups led to a generation of positive charge and appearance of the strong attractive forces between the anionic dye molecule and adsorbent surface (increase in removal percentage).

Optimization of CCD by DF for Extraction Procedure

The profile for the desirable option with predicted values in the STATISTICA 10.0 software was used for the optimization of the process (**Figure 5**). Additional experiments at the derived optimal conditions were conducted in three replicates to validate the optimum point of the factors. The level of each process parameters, optimal response values and experimental results are shown in **Figure 5** which optimum conditions were pH 6.0, sonication (5 min), adsorbent mass (0.025 g) and suggest that 12 mg L^{-1} of both dyes which supply maximum removal percentage. The optimum conditions were checked experimentally by running eleven experiments under the same conditions at 25 ^{0} C. The results showed an average dye removal efficiency of 98.20%. This is a high degree of agreement between the experimental and prediction indicating that the central composite design could be used effectively for the evaluation and optimization of the effects of the adsorption independent variables on the removal efficiency of dyes from aqueous solution using Au-Fe3O4 -NPs-AC.

Adsorption Equilibrium Study

The experimental adsorption equilibrium data were evaluated for studying the mechanism of BB and TB dyes adsorption onto Au-Fe3O4 -NPs-AC using different models such as Langmuir, Freundlich, Temkin, Dubinin–Radushkevich isotherms [31, 32, 33] in their conventional linear form. Subsequently, their corresponding constants were evaluated from the slopes and intercepts of respective lines (**Table 3**). These models were applied at two dosages of adsorbent while other variables were kept in optimal condition (**Table 3**). Fitting the experimental data to these isotherm models and considering the higher values of correlation coefficients (R2 = 0.999) for both dye, it was concluded that the Langmuir isotherm is the best model to explain the BB and TB dyes adsorption onto Au-Fe3O4 -NPs-AC, which quantitatively describes the formation of a monolayer of adsorbate on the outer surface of the Au-Fe3O4 -NPs-AC. It also shows the equilibrium distribution of metal ions between the solid and liquid phase.

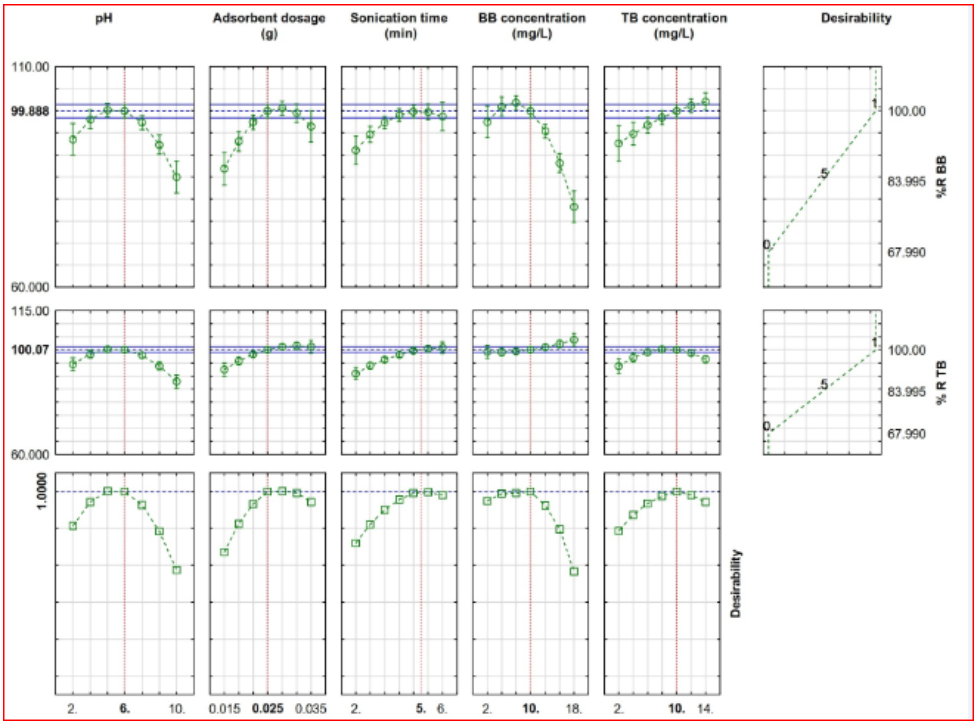

Figure 5. Profiles for predicated values and esirability function for removal percentage of BB and TB. Dashed line indicates current values after optimization

Table 3. Various isotherm constants and their correlation coefficients calculated for the adsorption of BB and TB onto Au-Fe3O4 -NPs-AC

Isotherm	Equation	Parameters	Value of parameters for BB	Value of parameters for TB
Langmuir	$q_e = q_m bC_e/(1+bC_e)$	Q_m(mg g^{-1})	80	76.38
		K_a (L mg^{-1})	10.49	1.344
		R^2	0.99	0.97
Freundlich	$\ln q_e = \ln K_F + (1/n) \ln C_e$	1/n	3.81	3.96
		K_F (L mg^{-1})	9.44	4.67
		R^2	96	0.93
Tempkin	$q_e = B_1 \ln K_T + B_1 \ln C_e$	B_1	15.55	10.63
		K_T (L mg^{-1})	106.75	9.3
		R^2	0.98	0.94
Dubinin-Radushkevich (DR)	$\ln q_e = \ln Q_s - B\varepsilon^2$	Q_s (mg g^{-1})	60.35	29.135
		B	6E-07	5E-07
		E (kj mol^{-1})	8535.53	3354.1
		R^2	0.97	0.93

Kinetic Study

The kinetic of reactions is strongly influenced by several parameters related to the state of the solid and to the physicochemical conditions under which sorption occurs. To investigate the BB and TB adsorption onto the adsorbent was checked using different kinetics models such as pseudo-first order [34], pseudo-second-order [35], Elovich [36] and intraparticle diffusion [37] models were studied [38-40] and accordingly constant and information corresponding to each model is given in **Table 4.** The regression coefficient (R^2) from pseudo-second order rate equation for adsorbent is higher when compared to the pseudo-first order equation. These results revealed that the kinetics of both dyes onto adsorbent exhibited best fit to the pseudo-second order equation for BB and TB dye by Au-Fe3O4 -NPs-AC.

Table 4. Various Kinetic constants and their correlation coefficients calculated for the adsorption of BB and TB onto Au-Fe3O4 -NPs-AC

Model	parameters	BB	TB
pseudo-First-order	k_1(min^{-1})	1.43	0.987
	qe (calc) (mg g^{-1})	10.155	17.92
	R^2	0.95	0.95
pseudo-Second-order	k_2 (min-1)	0.507	0.154
	q_e(calc) (mg g^{-1})	53.46	56.15
	R^2	0.999	0.999
Intraparticle diffusion	K_{diff} (mg g^{-1} min$^{-1/2}$)	4.59	8.05
	C (mg g^{-1})	40.71	33.77

Table 5. Comparison for the removal of dyes by different methods and adsorbents

Adsorbent	Adsorbate	Time (min)	Sorption capacity (mg g^{-1})	Ref.
Magnetically modified spent coffee grounds	BB	90	69.2	[41]
Magnetic fluid modified peanut husks	BB	90	95.3	[41]
Modified Form Iron Oxide Nanosphere	BB	1440	54.9	[42]
Iron Oxide Nanosphere	BB	1440	33.8	[42]
Mn-Fe_2O_4- NPs-AC	BB	10	70.3	[43]
Mn-Fe_2O_4- NPs-AC	TB	10	48.48	[43]
Au-Fe_3O_4 NPs-AC	BB	5	80	This Work
Au-Fe3O4 NPs-AC	TB	5	76.3	This Work

Comparison of Various Adsorbent

The performance of the proposed method has been compared with other adsorbents (**Table 5**). The adsorption capacity and contact time for present work are superior for other adsorbents BB and TB removal [41–43]. The results indicated that the ultrasound-assisted removal method has good ability to improve the efficiency of dyes removal. The ultrasonic-assisted enhancement of dye removal could be attributed to the high-pressure shock wave sand high speed microjets during the violent collapse of cavitations bubbles.

CONCLUSION

In the present study, Au –Fe3O4 – NP-AC were produced and tested as adsorbents for the removal of BB and TB dyes from aqueous samples. CCD was applied to evaluate the interactive effects of adsorption variables and optimize the adsorption process. The RSM combined with CCD suggest best operational conditions as follow: 5 min sonication, 0.025 g Au-Fe_3O_4 -NPs-AC, 12 mgL^{-1} for both dye and PH of 6. Langmuir isotherm gave a better fit to adsorption isotherms than Freundlich, Temkin and D–R isotherms using linear and nonlinear methods for prediction removal of dyes. The Langmuir is the best model for fitting experimental data, maximum adsorption capacity due to its higher R^2 value with 80.0, 76.3 mg g–1 for BB and TB dyes, respectively. The data indicate that the adsorption kinetics follow the pseudo-second-order rate in addition to inter particle diffusion for all analytes in binary system.

ACKNOWLEDGEMENT

The author expresses their appreciation to the Science and Research Branch Islamic Azad University, Tehran, Iran for financial support of this work.

REFERENCES

1. Baldikova E, Safarikova M, Safarik I. Organic dyes removal using magnetically modified rye straw. J. Magn. Mater. 2015;380:181-5.
2. Maleki A, Mahvi AH, Ebrahimi RY, Zandsalimi. Study of photochemical and sono chemical processes efficiency for degradation of dyes in aqueous solution. Korean. J. Chem. Eng. 2010;27:1805–10.
3. Gholami F, Borujeni A, Mahvi H, Naseri S, Faramarzi MA, Nabizadeh R, Alimohammadi M. Application of immobilized horseradish peroxidase for removal and detoxification of azo dye from aqueous solution. Res. J. Chem. Environ. 2011;15:217-22.

4. Ashrafi SD, Rezaei S, Forootanfar H, Mahvi AH, Faramarzi MA. The enzymatic decolorization and detoxification of synthetic dyes by the laccase from a soil-isolated as comycete Paraconiothyrium variable. Int. Biodeterio. Biode-grad. 2013;85:173–81.
5. Shirmardi MAH, Mahvi B, Hashemzadeh Naeimabadi A, Hassani G, Niri MV. The adsorption of malachitegreen (MG) asacationic dye on to functionalized multi walled carbon nano tubes. Korean. J. Chem. Eng. 2013;30:1603–8.
6. Jin Y, Wu Y, Cao J, Wu Y. Optimizing decolorization of methylene blue and methyl orange dye by pulsed discharged plasmain water using response surface methodology. J Taiwan Inst. Chem Eng. 2014;45:589–95.
7. Treviño-Cordero H, Juárez-Aguilar L, Mendoza-Castillo D, Hernández-Montoya V, Bonilla-Petriciolet A, Montes-Morán M. Synthesis and adsorption properties of activated carbons from bio mass of Prunusdomestica and Jacar and amimosifolia for the removal of heavy metals and dyes from water. Ind Crops Prod. 2013;42:315–23.
8. Ghaedi M, Karimi F, Barazesh B, Sahraei R, Daneshfar A. Removal of Reactive Orange12 from aqueous solutions by adsorptionon tinsulfide nanoparticle loaded on activated carbon. J. Ind Eng Chem. 2013;19:756–63.
9. Shin CH, Bae JS. Astability study of an advanced co-treatment system for dye wastewater reuse. J. Ind EngChem. 2012;18:775–9.
10. Abbasi AR, Akhbari K, Morsali A. Dense coating of surface mounted CuBTC Metal–Organic Framework nanostructures on silk fibers, prepared by layer-bylayer method under ultrasound irradiation with antibacterial activity. Ultrason. Sonochem. 2012;19:846–52.
11. Khanjani S, Morsali A. Ultrasound-promoted coating of MOF-5 on silk fiber and study of adsorptive removal and recovery of hazardous anionic dye ''congo red". Ultrason. Sonochem. 2014;21:1424–9.
12. Jamshidi M, Ghaedi M, Dashtian K, Hajati S, Bazrafshan A. Ultrasound assisted removal of Al 3+ ions and Alizarin red S by activated carbon engrafted with Ag nanoparticles: central composite design and genetic algorithm optimization. RSC Adv. 2015;5:59522–32.
13. Jamshidi M, Ghaedi M, Dashtian K, Hajatim S. New ion-imprinted polymer functionalized mesoporous SBA-15 for selective separation and pre concentration of Cr(iii) ions: modeling and optimization, RSC Adv. 2015;5:105789–99.
14. Asfaram A, Ghaedi M, Hajati SA, Goudarzi. Ternary dye adsorption ontoMnO2 nanoparticle-loaded activated carbon: derivative spectrophotometry and modeling. RSC Adv. 2015;5,72300–20.
15. Alipanahpour E, Ghaedi M, Asfaram A, Goudarzi A. Synthesis and characterization of ZnO-nanorods loaded onto activated carbon and its application for efficient solid phase extraction and determination of BG from water samples by micro volume spectrophotometry, New J. Chem. 2015;39:9407–9414.
16. Hajati S, Ghaedi M, Karimi F, Barazesh B, Sahraei R, Daneshfar A. Competitive adsorption of direct yellow 12 and reactive O12 on ZnS:Mn nanoparticles loaded on activated carbon as novel adsorbent. J. Ind. Eng. Chem. 2014;564-571.
17. Ghaedi M, Khajehsharifi H, HemmatiYadkuri A, Roosta M, Asghari A. Oxidized multiwalled carbon nanotubes as efficient adsorbent for bromothymol blue. Toxicol. Environ. Chem. 2012;94:873–883.
18. Taghizadeh F, Ghaedi M, Kamali K, Sharifpour ER, Sahraie Purkait MK. Comparison of nickel and/or zinc selenide nanoparticle loaded on activated carbon as efficient adsorbents for kinetic and equilibrium study of removal of Arsenazo (III) dye. Powder Technol. 2013;245:217–226.
19. Ghaedi M, Tashkhourian J, AmiriPebdani A, Sadeghian B, Nami Ana F. Korean J. Chem. Eng. 2011;28:2255–2261.
20. Ghaedi M, Hassanzadeh A, Nasiri Kokhdan S. Multiwalled Carbon Nanotubes as Adsorbents for the Kinetic and Equilibrium Study of the Removal of Alizarin Red S and Morin. J. Chem. Eng. Data. 2011;56:2511–2520.
21. Ghaedi M, Ansari A, Sahraei R. ZnS:Cu nanoparticles loaded on activated carbon as novel adsorbent for kinetic, thermodynamic and isotherm studies of reactive orange 12 and direct yellow 12 adsorption. Spectrochim Acta A. 2013;114:687-694.
22. Ghaedi M, Khaje Sharifi H, Hemmati Yadkuri A, Roosta M, Sahraei R, Daneshfar A. Spectrochim Acta A. 2012;86:62–8.
23. Bagheri S, Aghaei H, Ghaedi M, Asfaram A, Monajemi M, Bazrafshan AA. Synthesis of nanocomposites of iron oxide/gold (Fe3O4/Au) loaded on activated carbon and their application in water treatment by using sonochemistry: Optimization study. Ultrasonics – Sonochemistry. 2018;41:279–87.
24. Liu Y, Cui G, Luo C, Zhang L, Guo Y, Yan S. RSC Adv. 2014;4:55162–72.
25. Asfaram A, Ghaedi M, Hajati S, Goudarzi A, Bazrafshan AA. Spectrochim Acta, Part A. 2015;145:203-12.
26. Bagheri AR, Ghaedi M, Asfaram A, Bazrafshan AA, Jannesar R. Comparative study on ultrasonic assisted adsorption of dyes from single system onto Fe3O4 magnetite nanoparticles loaded on activated carbon: Experimental design methodology. UltrasonicsSono chemistry. 2016;34:294-304.

27. Hashemi P, Beyranvand S, Siah Mansur R, Ghiasvand AR. Anal. Chim.Acta. 2009;655:60–5.
28. Ghaedi M, Shahamiri M, Hajati Mirtamizdoust SB. J. Mol. Liq. 2014;199:483-88.
29. Montgomery DC. Design, Analysis of Experiments, 7th ed., John Wiley & Sons, Inc., Hoboken, NJ. 2007.
30. Jeong SY, Lee JW. Optimization of pretreatment condition for ethanol production from oxalic acid pretreated biomass by response surface methodology. Ind. Crop. Product. 2016;79 :1–6.
31. Ghaedi M, Hassanzadeh A, Kokhdan SN. J. Chem. Eng. Data. 2011;56:2511–20.
32. Ghaedi M, Sadeghian B, Pebdani AA, Sahraei R, Daneshfar A, Duran C. Chem. Eng. J. 2012;187:133–41.
33. Hajati S, Ghaedi M, Barazesh B, Karimi F, Sahraei R, Daneshfar A, Asghari A. J. Ind. Eng. Chem. 2014;20:2421–7.
34. Bello OS, Siang TT, Ahmad MA. Adsorption of Remazol Brilliant Violet-5R reactive dye from aqueous solution by cocoa pod husk-based activated carbon: kinetic, equilibrium and thermodynamic studies. Asia-Pacific Journal of Chemical Engineering. 2012;7:378-88.
35. Gupta H, Gogate PR. Intensified removal of copper from waste water using activated watermelon based biosorbent in the presence of ultrasound. Ultrason Sono chem. 2016;30:113-22.
36. Jamshidi M, Ghaedi M, Dashtian K, Hajati S, Bazrafshan AA. Sonochemical assisted hydrothermal synthesis of ZnO: Cr nanoparticles loaded activated carbon for simultaneous ultrasound-assisted adsorption of ternary toxicorganic dye: Derivative spectrophotometric, optimization, kinetic and isotherm study, UltrasonicsSonochemistry. 2016;32:119-31.
37. Alipanahpour E, Ghaedi M, Ghaedi A, Asfaram A, Jamshidi M, Purkait MK. Application of artificial neural network and response surface methodology for the removal of crystal violet by zinc oxide nanorods loaded on activate carbon: kinetics and equilibrium study. Journal of the Taiwan Institute of Chemical Engineers. 2016;59:210-20.
38. Weber WJ, Morris JC. Kinetics of adsorption on carbon from solution. J. Sanit. Eng. Div. 1963;89:31–60.
39. Safarik I, Katerina H, Barbora S, Safarikova M. Magnetically modified spent coffee grounds for dyes removal. Eur Food Res Technol. 2012;234:345-50.
40. Azad FN, Ghaedi M, Dashtian K, Hajati S, Pezeshkpour V. Ultrasonically assisted hydrothermal synthesis of activated carbon–HKUST-1-MOF hybrid for efficient simultaneous ultrasound-assisted Removal of ternary organic dyes and antibacterial investigation: Taguchi optimization. Ultrason Sono chem. 2016;31:383–93.
41. Safarik I, Safarikova M. Magnetic fluid modified peanut husks as an adsorbent for organic dyes removal. Physics Procedia. 2010;9:274-8.
42. Khosravi M, Yahyaei B, Azizian S. Adsorption of Bismarck Brown by Iron Oxide Nanosphere and Its Modified Form. Journal of Dispersion Science and Technology. 2014;1532-2351.
43. Bagheri S. Application of response surface methodology to modeling and optimization of removal of Bismarck Brown and Thymol Blue by Mn-Fe2O4- NPs-AC: Kinetics and thermodynamic studies. Oriental Journal of Chemistry. 2016;32.